Biochimica et Biophysica Acta 1850 (2015) 657–666

Contents lists available at ScienceDirect

Biochimica et Biophysica Acta

journal homepage: www.elsevier.com/locate/bbagen

A pore forming peptide from spider *Lachesana* sp. venom induced neuronal depolarization and pain

Masayoshi Okada [a,*], Gerardo Corzo [b], Gustavo A. Romero-Perez [a], Fredy Coronas [b], Hiroko Matsuda [a], Lourival D. Possani [b]

[a] Department of Pysiology, Kansai Medical University, Hirakata, Osaka 573-1010, Japan
[b] Departamento de Medicina Molecular y Bioprocesos, Instituto de Biotecnología, Universidad Nacional Autónoma de México, Cuernavaca, Morelos 62210, Mexico

ARTICLE INFO

Article history:
Received 10 July 2014
Received in revised form 12 November 2014
Accepted 28 November 2014
Available online 5 December 2014

Keywords:
Arachnoid venom
Depolarization
Inwardly rectifying K^+ channel (Kir2.1)
Pain
Pore-forming peptide
Thermal hyperalgesia

ABSTRACT

Background: Arachnoid venoms contain numerous peptides with ion channel modifying and cytolytic activities.
Methods: We developed a green fluorescent protein (GFP)-based assay that can monitor the changes in currents through overexpressed inwardly rectifying K^+ channels (Kir2.1), in which GFP expression was increased by blockade of Kir2.1 current. Using this assay, we screened venom of many spider species. A peptide causing GFP decreasing effect was purified and sequenced. Electrophysiological and pain-inducing effects of the peptide were analyzed with whole-cell patch-clamp recordings and hot-plate test, respectively.
Results: Among venoms we screened, soluble venom from *Lachesana* sp. decreased the GFP expression. Purification and sequencing of the peptide showed that the peptide is identical to a pore-forming peptide purified from *Lachesana tarabaevi* venom. Whole cell patch-clamp recordings revealed that the peptide had no effect on Kir2.1 current. Instead, it induced a current that was attributable to the pore-formation of the peptide. The peptide was selectively incorporated into hyperpolarized, i.e., Kir2.1 expressing, cells and for this reason the peptide decreased GFP expression in our Kir2.1 assay. The pore-formation positively shifted the reversal potential and induced burst firings in the hippocampal neurons in a synaptic current-independent way. The application of the *Lachesana* sp. peptide induced pain-related behavior in mice.
Conclusions: The peptide, which was found in *Lachesana* sp. venom, formed pores and thereby depolarized neurons and induced pain.
General significance: Our data suggested an additional physiological role of the pore-forming peptides.

1. Introduction

Arachnoid venoms contain numerous peptides with various functions for their survival. For instance, many blockers and openers for ion channels have been found [1,2]. Venom Ca^{2+} channel blockers and glutamate receptor blockers impair transmission at neuromuscular junction of preys, facilitating their capture by the spider. Furthermore, venom Na^+ channel openers and K^+ channel blockers depolarize the peripheral sensory neuron and induce pain to deter predators [2–4]. In addition, several arachnoid venoms, especially from wolf-spiders, contain a significant amount of pore-forming peptides, which have cytolytic activities [5–7]. These peptides are shown to be inserted into membrane forming a pore, which lead to necrotic and antimicrobial effects [2].

Inwardly rectifying K^+ channel (Kir2.1) is expressed in heart, smooth muscle, and central and peripheral nerve cells [8]. Physiological importance of Kir2.1 is shown by severe phenotype of its mutation [9]. But no peptide blockers have been found for Kir2.1 so far. We have prepared lentiviral vector which expresses Kir2.1 using 293T cells as virus producer, for the investigation of its neuronal role [10]. In our production system of lentiviral vectors, both Kir2.1 and green fluorescent protein (GFP) were expressed in the 293T cells during viral production. We found that the excessive expression of Kir2.1 resulted in degeneration of viral vector producing cells. Conversely, blockade of Kir2.1 current prevented the degeneration and increased the production ability (Okada et al., submitted). This finding implies that the blockade of Kir2.1 current can be monitored with GFP coexpression, which may be applicable to a high-through-put assay for Kir2.1.

In this report, we looked for novel K^+ channel modifiers and we established a GFP-based assay for Kir2.1. Using this assay, we screened arachnoid venoms, and found a peptide that had GFP decreasing effect. Unexpectedly, this peptide did not affect the Kir2.1 current itself, but formed pores in a Kir2.1 current-dependent way. The pore formation depolarized cells and induced burst firings in the hippocampal neurons. An application to mouse paw induced pain-related behavior, suggesting a new physiological role of pore-forming peptides.

* Corresponding author at: 2-5-1, Shin-machi, Hirakata, Osaka 573-1010, Japan. Tel.: +81 72 804 2321; fax: +81 72 804 2329.
E-mail address: mokada-tky@umin.ac.jp (M. Okada).

http://dx.doi.org/10.1016/j.bbagen.2014.11.022
0304-4165/

2. Materials and methods

2.1. GFP-based assay for Kir2.1

cDNA of Kir2.1 was generously donated by Dr. Jan (UCSF). The expression vector, CS-β-actinP-GFP-IRES-Kir2.1 (Fig. 1A), was constructed from CS-CDF-CG-PRE, which was donated by Dr. Miyoshi (Riken, Ibaraki, Japan), and the CMV promoter was replaced with that of chicken β-actin. Internal ribosomal entry site (IRES) was inserted between cDNAs of hrGFP (Stratagene, La Jolla, CA) and Kir2.1 to enable the coexpression of the two proteins. Woodchuck hepatitis virus post-transcriptional regulatory element (WPRE) was attached to the 3′ of Kir2.1, to enhance expression. D172G/E224S mutations were made with PCRs. The pmCherry-C1 plasmid (Clontech, Mountain View, CA) was used to express a red fluorescent protein (mCherry), which served as control.

293T cells were cultivated in 6-well plate (approximately 1200–1400 cells/mm^2) in DMEM supplemented with 10% FBS. Cells were transfected by three micrograms of the plasmid with calcium-phosphate method, and were washed twice with phosphate-buffered saline (PBS) 5 h after [11]. Then, medium containing venom fraction was added to each well. Cells were washed with PBS and fixed with 4% paraformaldehyde 48 h after transfection, and the fluorescence was measured with a plate reader (Infinite200, Tecan, Männedorf, Switzerland). The expressions of fluorescent proteins were indicated as the arbitrary units of the plate reader.

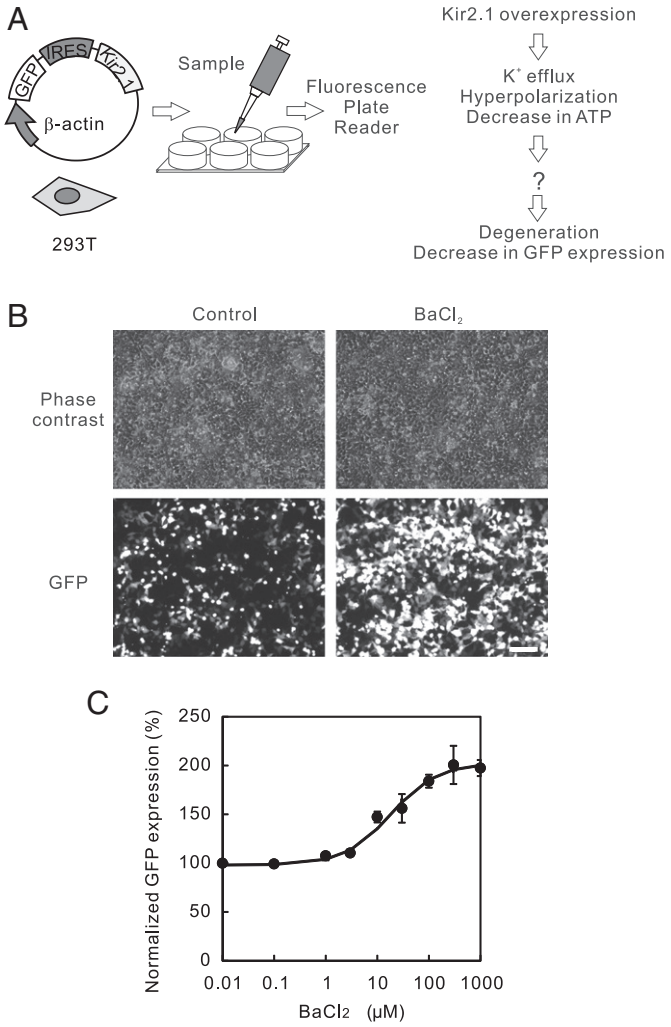

Fig. 1. GFP-based assay for Kir2.1 current and following processes. (A) Schematic illustration of the GFP-based assay. After transfection of CS-β-actinP-GFP-IRES-Kir2.1 plasmid to 293T cells, venom samples were added to the medium. The overexpression of Kir2.1 resulted in degeneration and decrease in GFP expression, probably through detachment of degenerative cells and decrease in ATP level. (B) Phase contrast and GFP fluorescence images of Kir2.1 expressing 293T cells. The phase contrast images show that there is no difference in total cell number, but GFP fluorescence was increased by addition of $BaCl_2$ (0.3 mM). Whereas control cells are degenerative, $BaCl_2$-treated cells mostly look healthy. These images were taken 48 h after transfection. Bar = 100 μm. (C) $BaCl_2$ concentration-dependent increase in GFP expression. Transfected cells were incubated with various concentrations of $BaCl_2$. Expressions of GFP were measured with a plate reader 48 h after. Each data point indicates mean and SEM of four experiments and was fitted to Hill equation 4 parameters with clamp-fit software (Axon Instruments).

2.2. Preparation, purification, and sequencing of Lachesana sp. venom

Lachesana sp. crude venom (4 mg) obtained from the Republic of Kazakhstan (Fauna Laboratories Ltd., Almaty, Kazakhstan) was resuspended in 0.1% aqueous TFA, and the insoluble material was removed by centrifugation at 14,000 ×*g* for 5 min. The supernatant (whole soluble venom) was used directly for HPLC separation. The diluted venom was fractionated using a reverse-phase semipreparative C_{18} column (5C_{18}MS, 10 × 250 mm, Vydac, Hesperia, CA, USA) equilibrated in 0.1% TFA, and eluted with a linear gradient of acetonitrile from 0 to 60% in 0.1% TFA, run for 60 min at a flow rate of 2 mL/min as described previously [12]. Effluent absorbance was monitored at 230 nm. Fractions were collected in 1.5 mL plastic vials and dried out under high vacuum. Peptide fractions decreasing GFP expression (see below) were subjected to a final step of purification performed by an analytical C_{18} reverse-phase column (4.6 × 250 mm, Vydac, Hisperia, CA, USA) equilibrated in 0.1% TFA, and eluted with a linear gradient of acetonitrile from 20 to 60% in 0.1% TFA, run for 40 min at a flow rate of 1 mL/min. The pure component was analyzed by direct sequencing of the native toxin (Edman degradation), using a Shimadzu PPSQ-31A (Shimadzu, Kyoto, Japan) automated gas-phase sequencer. Samples were dissolved in 10 μl of a 37% acetonitrile (v/v) solution and applied to TFA-treated glass fiber membranes, precycled with Polybrene (Aldrich, St. Louis, MO). Data were analyzed using the Shimadzu PPSQ-31A software. The theoretical mass was confirmed by electro spray ionization mass spectrometry using a LCQ DUO ion trap mass spectrometer (Finnigan, San Jose, CA) with and ESI source from 2.1 to 3.1 kV.

After N-terminal sequencing, *Lachesana* sp. Fraction 26 peptide was chemically synthesized (Peptide 2.0 Inc., Chantilly, VA). Css54, a pore-forming peptide obtained from the venom of the scorpion *Centruroides suffusus suffusus*, was used as positive control and it was chemically synthesized in our laboratory [13]. The concentration of native peptides was determined according to the absorbance at 230 nm, but chemically synthesized peptides were measured by dry weight.

To discuss the evolution of pore-forming peptides, a cladogram was built based on their amino acid homology using a Neighbor-joining method without distance corrections algorithm. Isoelectric points (PI) of the peptides were calculated using pK values of amino acids described at http://us.expasy.org/tools/pi_tool.html.

2.2.1. Fluorescnt labeling of LaFr26

Eighty micrograms of synthetic LaFr26 was dissolved in 80 μl of fresh 0.5 M $NaHCO_3$ (pH 8.5). To this solution, a freshly prepared solution of 50 nmol of Tetramethylrhodamine isothiocyanate isomer R (TRITC, Sigma, MO) in 20 μl of dimethylformamide was added. The molar ratio peptide: TRITC was 1:5 in order to label few primary amine residues. The mixture was incubated for 1 h at room temperature, and it was separated by reversed-phase HPLC chromatography using an analytical C_{18} reverse-phase column (4.6 × 250 mm, Vydac, Hisperia, CA, USA) equilibrated in 0.1% TFA, and eluted with a linear gradient of acetonitrile from 20 to 60% in 0.1% TFA, run for 40 min at a flow rate

of 1 mL/min. The unreacted and the labeled peptide were identified by mass spectrometry.

For the labeled peptide incorporation experiment, 293T cell and 56-3 cell, which was derived from 293T cell and stably express Kir2.1 and GFP with a lentiviral vector [10], were mixed (approximately 1:1) and incubated for 24 h in a same 35 mm dish. We then added the labeled peptide and fixed the cells with 4% paraformaldehyde 10 min after. Single plane confocal images were taken (FV300, Olympus, Tokyo, Japan).

2.3. Patch-clamp recordings from 293T cells

For patch-clamp recordings, we used 293T and 56-3 cells. The coverslip containing grown cells were transferred to a recording chamber (2 × 0.5 × 0.2 cm, 200 μL in volume) set on the stage of an inverted microscope (Olympus IX71, Tokyo, Japan). We perfused (50 μL/min) Tyrode solution containing (in mM): NaCl 140, KCl 5.4, NaH_2PO_4 0.33, $CaCl_2$ 2, $MgCl_2$ 1, HEPES 5, and glucose 5.5 (pH 7.4). Using a micro pipet, we gently applied the peptide solution to an adjacent reservoir pool, of which volume is negligible, and kept perfusing even after venom application to maintain water level. We recorded whole-cell currents using an Axopatch 200B amplifier (Axon Instruments, Foster City, CA) at 25.0 ± 1.0 °C. Patch pipettes pulled from borosilicate glass (Narishige, Tokyo, Japan) were filled with an internal solution containing (in mM): thyc=10?>K-aspartate 66, KCl 71.5, KH_2PO_4 1, EGTA 5, Hepes 5, and K_2ATP 3 (pH 7.4 adjusted with KOH). Typical pipette resistance was 4 MΩ. Records were digitized at 10 kHz, and low-pass filtered at 2 kHz. Ramp or step pulses were applied from a holding potential of −70 mV, unless written in text. Whole-cell conductance was calculated with a step pulse from −40 to −20 mV or −90 to −70 mV. Liquid-junction potentials were not compensated in either recording from 293T or hippocampal cells.

2.4. Slice patch-clamp recordings and immunostaining of organotypic culture of hippocampus

Hippocampal slices were cultured as described previously [10], on the approval of the animal experiment committee of Kansai Medical University. The hippocampi prepared from P7 rats were sliced (350 μm in thickness) with a McIlwain chopper, and cultivated on a Millicell-org (Millipore, Billerica, MA) at 34 °C for 9–18 days.

For the patch-clamp recordings, we transferred the slice to an upright microscope (BX51WI, Olympus) and perfused with artificial cerebrospinal fluid (aCSF), which contained (in mM): NaCl 131, KCl 2.75, NaH_2PO_4 1.1, $NaHCO_3$ 26, glucose 12, $CaCl_2$ 2, and $MgCl_2$ 1, and was equilibrated with 95% O_2–5%, CO_2 (pH 7.4). Using the same amplifier, whole-cell recordings were made from the CA1 pyramidal neurons visually identified with a Nomarski objective. The internal solution was the same as that used for 293T cells.

For the c-fos immunostaining, LaFr26 peptide (3 μM), dissolved in PBS, was injected to the extracellular space of the CA3 pyramidal layer using Femtojet and Femtotip (0.1 s, 200 hPa, Eppendorf, Hamburg, Germany). The slices were incubated at 34 °C for 1 h and then fixed with 4% paraformaldehyde. The slices were incubated with a primary antibody against c-fos (Santa Cruz, Santa Cruz, CA) for 48 h at 4 °C. The immunoreaction was visualized with secondary antibody labeled with Alexa 488 (Molecular Probes, Eugene, OR). Multi-plane images were taken with a confocal microscope (FV300) and overlayed.

2.5. Hot-plate test

Male CD-1 mice (4–5 weeks, 18–22 g) were housed in cages with a 12/12-h light/dark cycle and constant room temperature (~25 °C), with standard laboratory food and water ad libitum. Each animal was used only once. A hot-plate test was used for measuring the pain-inducing, hyperalgesic, effect of LaFr6 and Css54 to an acute thermal stimulus [14]. Five mice per group were used and they were allowed to acclimate an hour before testing. Each group was subcutaneously injected into the plantar right hind paw (in a volume of 5 μL) with either 0.65 mg/kg mice of LaFr26, Css54, or a control solution of PBS. The drug vehicle for all experiments was PBS (pH 7.2). A 10 μL microsyringe (Hamilton syringe, fixed needle, 26 SG, bevel tip) was used for plantar injection to minimize the noxious stimuli. A single animal was placed in a plexiglass cylinder (20 × 25 cm) on the hot plate (Panlab model LE7406, Harvard Apparatus, Holliston, MA) maintained at 55 °C. The time taken for the animals to withdraw the paw from the hot-plate was recorded after placing the animal into the chamber, and the cutoff time was 30 s. Keterolac, a non-steroid analgesic, was used as an analgesic control. Animal groups were tested at 5, 10, 15 and 20 min post-injection. The protocols were performed in compliance with the ethics committee of the Instituto de Biotecnologia of the Universidad Nacional Autonoma de Mexico (UNAM), Campus Morelos and they were carried in accordance with the guidelines for the care of laboratory animals and the ethical guidelines for investigation of experiments in conscious animals. The number of animals and intensity of the noxious stimuli were the minimum necessary to demonstrate consistent effects of drug treatments. All efforts were made to minimize both animal numbers and suffering within the experiments. Results are shown as the mean ± SEM. The nociceptive effect of either LaFr26 or Css54 was statistically compared with the controls by two-way ANOVA, followed by Bonferroni post-test, where $p < 0.05$ was considered as significant, using the GraphPad Prism software.

3. Results

3.1. GFP-based assay for Kir2.1

In our preceding report [10], we constructed a plasmid that coexpressed Kir2.1 and GFP for preparation of lentiviral vector (Fig. 1A), and found that the expression of Kir2.1 current led to degeneration of cells (Okada et al., submitted). Therefore, we expected that this degenerative effect of overexpressed Kir2.1 might decrease the coexpression of GFP and thereby allow us to monitor the changes in Kir2.1 current with GFP fluorescence. To test this, we transfected the CS-β-actinP-GFP-IRES-Kir2.1 plasmid to 293T cells, and then the cells were incubated in the presence or absence of a Kir2.1-selective blocker, Ba^{2+} [15]. The morphology of the cells was examined 48 h after transfection. Phase contrast images show that the densities of both cells were high and the cells were confluent (Fig. 1B). But, expectedly, there was a difference in GFP expression. In the absence of $BaCl_2$, GFP-positive cells were round and shrunken, showing a typical degenerative morphology. The addition of $BaCl_2$ prevented the degenerative change, and importantly the GFP fluorescence was increased.

Therefore it may be feasible to use this change in GFP expression for a quantitative assay for Kir2.1 channel. To test the feasibility, we added various concentrations of $BaCl_2$ to the medium of CS-β-actinP-GFP-IRES-Kir2.1 plasmid transfected 293T cells, and incubated for 48 h. Subsequently, the GFP expression was measured with a fluorescence plate reader. The GFP expression was increased in a concentration-dependent way (Fig. 1C), and the EC_{50} (18.3 μM) was comparable to that determined with patch-clamp recordings (16.0 μM). These findings indicate that current through Kir2.1 channel can be monitored with the GFP expression, showing the feasibility of this GFP-based assay for the screening of Kir2.1 channel blockers.

At present, there are no available Kir2.1 channel openers, which increase channel conductance or reduce the inward rectification of the channel. Thus, it is difficult to test whether our assay can detect the possible Kir2.1 opener or not. Mutations of Kir2.1 D172G/E224S reduce the inward rectification and result in larger outward current [16,17]. Therefore expression of D172G/E224S mutant can mimic the effect of Kir2.1 opener. We then transfected CS-β-actinP-GFP-IRES-Kir2.1 and CS-β-actinP-GFP-IRES-Kir2.1 (D172G/E224S) plasmid, and measured expression of GFP. Expectedly, the GFP expression in the D172G/E224S

expressing cells was lower than that in wild-type (9177 ± 269 and 9868 ± 243 (arbitrary units of plate reader), n = 4, $p < 0.01$ Student's *t*-test), suggesting that this assay can also detect the increment in Kir2.1 current. We conclude that this assay is useful to detect both blockers and openers of Kir2.1 channel.

3.2. Screening of spider venoms and purification of GFP-decreasing activity

In order to find a new blocker or opener for Kir2.1, we next conducted a screening of crude arachnoid venoms of 33 species of scorpions and spiders. We transfected 293T cells grown in a 6-well plate with the CS-β-actinP-GFP-IRES-Kir2.1 plasmid, and then added whole soluble venoms dissolved in 2 mL of culture media (final concentration 10 μg/mL). The GFP expression was measured 48 h after. Whereas most of the venoms did not affect the expression, the venom of *Lachesana* sp. (10 μg/mL) decreased the GFP expression (Fig. 2A). To purify the active component, we fractionate the venom with a C_{18} reverse-phase HPLC column and assayed each fraction with the GFP-based assay (Fig. 2B and C). The GFP decreasing activity was found in fraction (Fr) 26 when applied at a concentration of 5 μg/mL.

3.3. Sequencing of Lachesana sp. Fr26

Mass spectrometry analysis showed that fraction 26 was pure (only one component) with a molecular mass of 7905.6 Da. The purified *Lachesana* sp. Fr26 peptide (LaFr26) was N-terminal sequenced using Edman degradation (Table 1), and found the first 58 residues. After enzymatic cleavage using Asp-N the last eleven residues were identified similarly. The theoretical and experimental molecular masses of LaFr26 corresponded with each other. We found that the LaFr26 peptide was identical to cyto-insectotoxin 1a (CIT1a) purified from *L. tarabaevi*

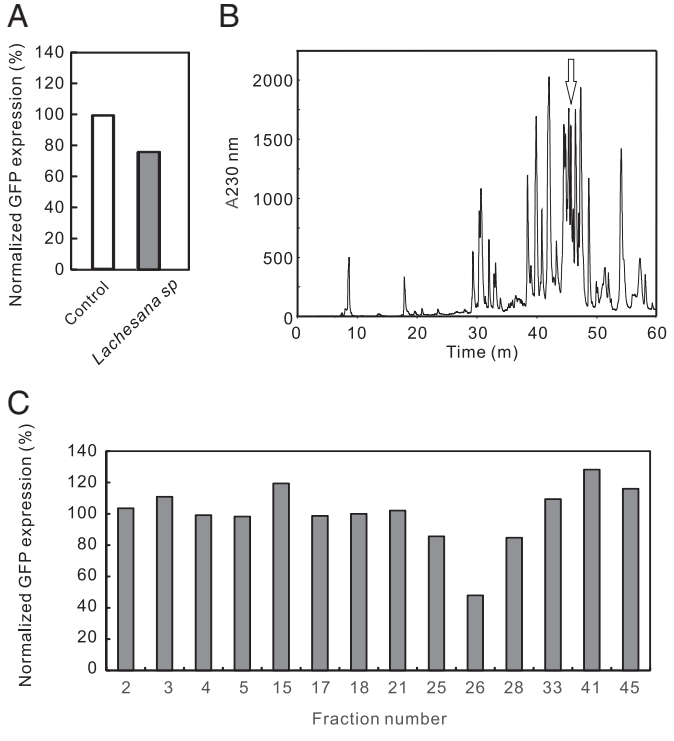

Fig. 2. Screening of *Lachesana* sp. venom with GFP-based assay. (A) Decrease in GFP expression by *Lachesana* sp. venom. GFP expression of 293T cells, which was incubated with *Lachesana* sp. venom, was measured and normalized to that of PBS control. Average of two experiments is shown. (B) HPLC chromatogram. The whole soluble venom was fractioned by a reverse-phase column. Ordinate indicates the $A_{230\ nm}$. The arrow indicates the peak of Fr26. (C) GFP-based assay of each fraction. Fractions separated by HPLC were applied to the GFP-based assay. Fractions, of which $A_{230\ nm}$ was low, were not assayed. (n = 2).

Table 1
Amino acid sequence of LaFr26 and related peptides from *Lachesana tarabaevi*.

Accession	Sequence	MW (Da)
LaFr26	GFFGNTWKKIKGKADKIMLKKAVKIMVKKEGISKEE AQAKV**DAMSKKQIRLYLLKYYGKKALQKASEKL**	7905.6
P85253	GFFGNTWKKIKGKADKIMLKKAVKIMVKKEGISKEE AQAKVDAMSKKQIRLYLLKYYGKKALQKASEKL	7905.6
P0CAZ7	GFFGNTWKKIKGKADKIMLKKAVKIMVKKEGISKEE AQAKVDAMSKKQIRLYLLKYYGKKLFKKRPKNCDQ	8295.1
P0CAZ3	GFFGNTWKKIKGKTDKIMLKKAVKIMVKKEGISKEE AQAKVDAMSKKQIRLYLLKHYGKKALQKASEKL	7909.6

Bold letters in LaFr26 represent N-terminal sequencing after enzymatic cleavage using Asp-N. Underlined letters indicate different amino acids from LaFr26. P85253, M-zodatoxin-Lt8a; P0CAZ7, M-zodatoxin-Lt8o; P0CAZ3, and M-zodatoxin-Lt8j from *Lachesana tarabaevi*.

[18,19]. Vassilevski et al. [19] reported several cationic peptides identified from the *L. tarabaevi* spider venom. Among them, CIT1a was the most abundant peptide and had cytolytic activity on bacteria, insect cells, and human erythrocytes and lymphocytes. They showed a concentration and voltage-dependent dye leaking activity of CIT1a on planar lipid bilayers.

3.4. Dose- and Kir2.1 current-dependent GFP decreasing effect of LaFr26

For further experiments, LaFr26 was chemically synthesized. Then to examine the concentration–response relationship of the peptide on GFP expression, we incubated the CS-β-actinP-GFP-IRES-Kir2.1-transfected cell with various concentrations of the chemically synthesized LaFr26. We observed a dose-dependent decrease in GFP expression (Fig. 3A). The EC_{50} and Hill coefficient were 2.89 μM and 1.66, respectively (n = 4).

To test whether this GFP expression decrement effect is dependent on Kir2.1 current or not, we incubated Kir2.1 expressing cells with 10 μM of LaFr26 peptide in the presence or absence of 0.3 mM $BaCl_2$ (Fig. 3B). The blockade of Kir2.1 current significantly reduced the decrement in GFP expression. We then tested the effect of LaFr26 on the cells that expressed only a red fluorescent protein, mCherry. LaFr26 had no effect on the expression of mCherry (Fig. 3C). These data suggest the Kir2.1 current-dependency of the GFP-decreasing effect of *Lachesana* sp. peptide.

To exclude the possibility of non-specific effect of synthetic peptides on this assay, we tested the effect of synthetic secretin peptide (27 amino acids, 10 μM). To our knowledge, there are no interactions between secretin and Kir2.1 or endogenous expression of secretin receptor in 293T cells. The addition had no effect on the GFP expression (Fig. 3D).

3.5. LaFr26 induced nonselective current without affecting Kir2.1 current

The Kir2.1 current-dependency suggests that LaFr26 peptide may be an opener for Kir2.1 channel. To clarify whether LaFr26 is an opener for Kir2.1 or not, we carried out patch-clamp recording from 56-3 cells. It is well-known that Kir2.1 channel is inhibited by intracellular cations, i.e., Mg^{2+} and spermine, in a depolarization-dependent way [20,21]. Therefore outward current decreases according to the depolarization (namely inward rectification). When we recorded whole-cell current under voltage-clamp mode and applied a ramp pulse from −150 to 10 mV, the outward current was inhibited and showed the bump-like shape as the cell was depolarized (Fig. 4A, 0 min). Then we applied 200 μL of 10 μM LaFr26 and recorded 1 min after. Unexpectedly, the peptide did not affect the current immediately after application (Fig. 4A, 1 min). Interestingly, four and seven minutes after application, the inward and outward currents were gradually increased and less inward-rectified (4 and 7 min). Ten minutes after (10 min), the currents became larger and the inward rectification was completely disappeared, suggesting an induction of different current.

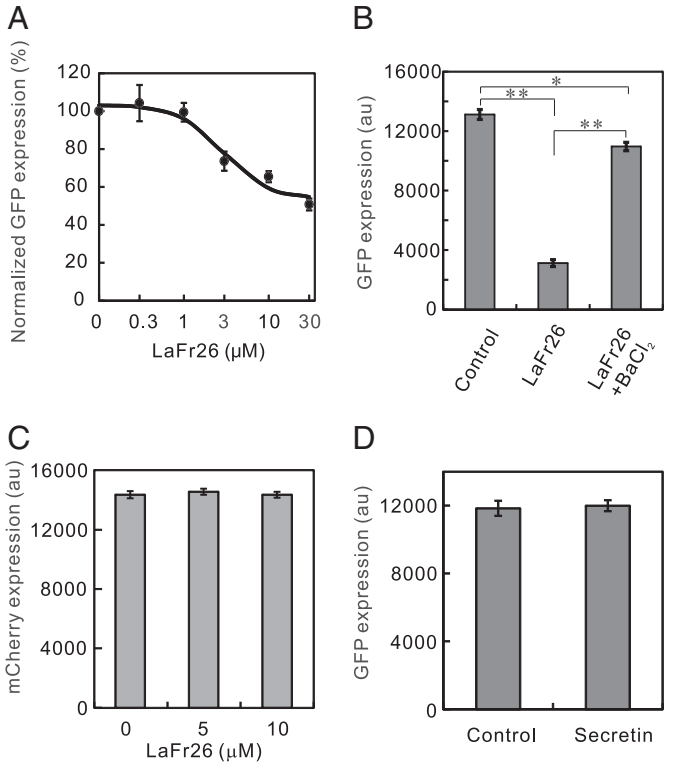

Fig. 3. Concentration- and Kir2.1 current-dependent decrease in GFP expression by LaFr26. (A) Concentration-dependent GFP decreasing effect of LaFr26. After the transfection with CS-β-actinP-GFP-IRES-Kir2.1 plasmid, 293T cells were incubated with various concentrations of LaFr26 peptide for 48 h. Each data point indicates mean and SEM of GFP expressions, which were normalized to that of PBS control, of four experiments, and the slope was fitted to the Hill equation. (B) Kir2.1 current dependent decrease in GFP expression. The transfected 293T cells were incubated with 10 μM of LaFr26 peptide in the presence or absence of 0.3 mM $BaCl_2$, and GFP expressions were measured 48 h after. Blockade of Kir2.1 current significantly reduced the GFP decreasing effect of LaFr26peptide. (* $p < 0.0005$, ** $p < 0.00001$, ANOVA followed by Student's *t*-test, $n = 4$). (C) Lack of effect of LaFr26 on the mCherry expression. The 293T cells were transfected with pmCherry-C1 plasmid, which express only mCherry, and were incubated with 0, 5, and 10 μM of LaFr26 peptide. mCherry expressions were not affected 48 h after ($n = 4$). (D) Lack of effect of secretin on the GFP expression. Addition of secretin (10 μM, Genscript, Piscataway, NJ) had no effect on the GFP expression in CS-β-actinP-GFP-IRES-Kir2.1 plasmid transfected cells ($n = 6$).

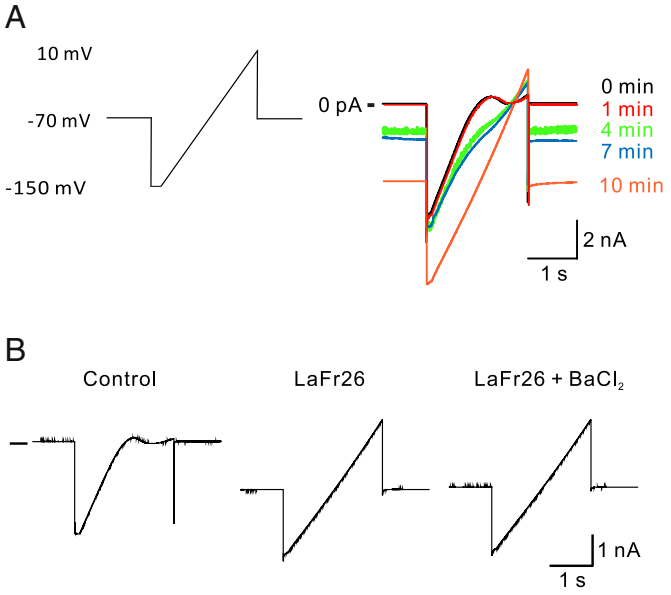

Fig. 4. Lack of effect on Kir2.1 current and induction of another current. (A) After the whole-cell patch-clamp was made from a 56-3 cell, we evoked Kir2.1 currents with a ramp pulse (left panel). Typical inwardly rectifying K^+ current was observed before the application of the peptide (0 min). Then we applied 200 μl of LaFr26 (10 μM) dissolved in Tyrode solution. Since the volume of the recording chamber is 200 μl, the extracellular solution was supposed to be fully replaced. The peptide did not affect the Kir2.1 current (1 min), and therefore the trace of 1 min completely overlapped with that of 0 min. Afterward, the I–V curve shifted rightward and the inward rectification became weaker (4 and 7 min). Ten minutes after the application, the holding and evoked currents became larger and no inward rectification was observed (10 min). (B) Typical Kir2.1 current was evoked before application of the peptide (Control). Ten minutes after application of 10 μM LaFr26 peptide, the current without inward rectification was induced (LaFr26). Then application of 200 μl of Tyrode solution containing 0.3 mM of $BaCl_2$ had no effect on the induced current (LaFr26 + $BaCl_2$). Bar in left indicates the position of 0 pA.

To confirm that the newly induced current is different from Kir2.1 current, we applied 0.3 mM of $BaCl_2$ after the current induction, and found that the induced current was resistant to Ba^{2+} (Fig. 4B). To further confirm the difference, we applied the peptide to naive 293T cell, which was voltage-clamped at −90 mV (see below), and found the induction of current as same as the Kir2.1 expressing cells (Fig. 5A). These results suggest that the LaFr26 peptide induced current was different from Kir2.1 current. We analyzed the reversal potential of the current with the ramp pulse and found that the reversal potential shifted from -79.8 ± 3.6 to -10.0 ± 2.5 mV (Fig. 5A, $n = 4$). Theoretical reversal potential for K^+ was −87.4 mV. Because internal solution did not contain Na^+ or Ca^{2+}, those for these ions were more positive. This result indicates that the LaFr26 induced current is not ion-selective.

3.6. Voltage-dependent pore formation of LaFr26 peptide

Reportedly, CIT1a peptide from *L. tarabaevi* venom is inserted into the cell membrane and assembles to form pores [18]. Taken together with our results, the induced current may be attributable to the current through the pore formed by the LaFr26 peptides. To confirm this possibility, we applied another pore-forming peptide, *C. suffusus suffusus* fraction 54 (Css54) [13] to 56-3 cells. The application also induced similar current, supporting the possibility of pore current (Fig. 8A). The induction was faster than that of LaFr26 peptide.

These results raised a question of why the GFP-decreasing effect was apparently dependent on Kir2.1 current. Namely, the GFP expression decreasing effect of LaFr26 was dependent on Kir2.1 current in our GFP-based assay (Fig. 3 B and C); but the peptide induced the pore current without affecting Kir2.1 current (Fig. 4). Possible explanation for this apparent dependency is that the pore-formation of the peptide is dependent on the membrane potential rather than Kir2.1 current itself. Because LaFr26 is a basic peptide, it is likely that the peptide is selectively inserted and/or assembled in hyperpolarized cells. Indeed, resting membrane potentials of control and Kir2.1 expressing cells were -44.8 ± 3.2 and -86.6 ± 1.1, respectively ($n = 8$). To test this possibility, we made whole-cell patch clamp with naive 293T cells and hold them at −40 or −90 mV. Then we applied 10 μM LaFr26 peptide and measured whole cell conductance. Expectedly the peptide increased conductance of the cells held at −90 mV, but not at −40 mV (Fig. 5A, B, and C).

To test whether the LaFr26 peptide was incorporated or assembled in the hyperpolarization-dependent way, we labeled the LaFr26 peptide with a red-fluorescent dye, TRITC. We also prepared the mixed culture of naïve 293T cells and 56-3 cells, which stably expresses GFP and Kir2.1. Then we added the labeled LaFr26 (1 μM) to the medium and incubated for 10 min at 37 °C. Red fluorescence was selectively observed in green fluorescence positive cells (Fig. 5D and E). Next we categorized as "LaFr26-positive," in which cell is evenly positive (arrows), or "LaFr26-negative," in which red fluorescence is negative or positive only partially (arrowhead). The percentage of TRITC-positive cells was significantly higher in the GFP-positive cells (Fig. 5F). Similar result was obtained with higher concentration of labeled LaFr26 peptide

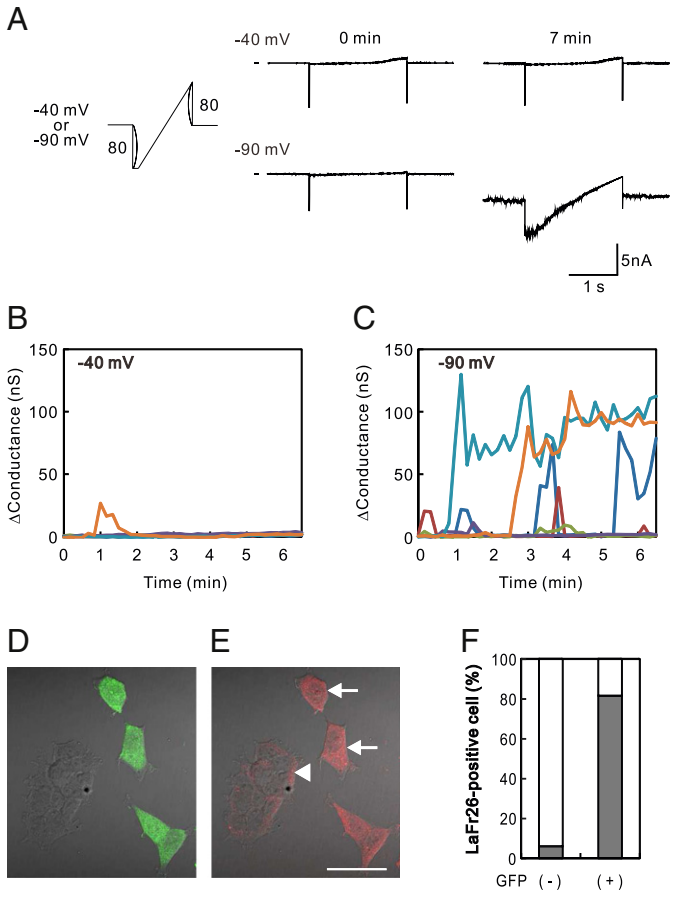

Fig. 5. Voltage-dependent pore formation of *Lachesana* sp. venom. (A) After whole cell patch-clamp was made, naive 293T cells were held at −40 or −90 mV. Then we recorded the current evoked by the ramp pulse (left panel). Typical traces at before (0 min) and 7 min after application of 200 μl of LaFr26 (10 μM) were shown. Naive 293T cell clamped at −40 mV endogenously expressed slight outward current. LaFr26 had no effect 7 min after application. But, in the cell clamped at −90 mV, the peptide induced the current. (B and C) Timecourse of whole cell conductance of six cells. Naive 293T cells were clamped at −40 or −90 mV and 200 μl of 10 μM LaFr26 was applied at time 0. Whole-cell conductance was measured by a step pulse (from −40 to −20 mV or from −90 to −70 mV, 0.2 s) every 10 s. Each data point represents the change in conductance from initial value. Data from 6 cells were overlayed. Whereas only one out of six cells showed changes in more than 10 nS at −40 mV, five cells showed the changes at −90 mV. (D, E, and F) Selective incorporation of LaFr26 into Kir2.1 expressing cells. Mixed culture of naïve 293T and 56-3 cells was incubated with TRITC-labeled LaFr26 for 10 min. Images of differential interference contrast (DIC) and green (D) or red (E) fluorescence were overlaid. Selective incorporation of labeled peptide in GFP-positive cells is seen. Bar 50 μm. (F) Percentage of the peptide incorporated cell (arrows) is significantly higher in the Kir2.1 expressing cells (n = 66, GFP-positive cells; n = 76, GFP-negative cells, $p < 0.00005$, χ^2-test).

(3 μM, data not shown). These results suggest the hyperpolarization-dependent incorporation into the Kir2.1 expressing cells.

3.7. LaFr26 peptide induced neuronal depolarization and firing

Voltage-clamp recordings showed that the application of *Lachesana* sp. peptide positively shifted the reversal potential to −10 mV (Fig. 4A), indicating a depolarizing effect of the peptide. To examine the depolarizing effect of LaFr26 peptide, we recorded membrane potential of 56-3 cells under the current-clamp configuration. After the application of LaFr26 (10 μM), whole cell membrane potential initially fluctuated and afterward the potential was abruptly depolarized to −15 mV and repolarized afterward (Fig. 6A).

If this is the case in neurons, neurons will fire according to the depolarization. To test this, we prepared the hippocampal slice culture, and made whole-cell current-clamp recordings from the CA1 pyramidal neurons. Initially the hippocampal slice was perfused with normal aCSF and the perfusate was switched to that containing 1 and 10 μM of LaFr26 sequentially. Expectedly, the application of 10 μM peptide increased the firing rate (Fig. 6B). Similar firings were observed in six out of seven neurons. The burst firings were followed by the sustained depolarization (about −20 mV) and inactivation. This inactivation is probably attributable to the steady-state inactivation of Na^+ channel.

Reportedly, a component of black widow spider venom enhances neurotransmitter release [22]. Therefore increase in firing can be explained by two possibilities: direct depolarization in post-synaptic neuron, or indirect depolarization through enhanced release of neurotransmitters and following facilitated synaptic inputs. To test the latter possibility, we added antagonists for glutamate and $GABA_A$ receptors, i.e., NBQX (20 μM), AP-5 (25 μM), and bicuculline (10 μM) to the aCSF. The addition of antagonists completely abolished spontaneous firings (Fig. 6C). We then added the LaFr26 peptide to the perfusate. The neuron was abruptly depolarized and fired frequently. Afterward, the neuron became inactivated, and the membrane potential was remained at about −20 mV.

To confirm the neuronal depolarizing effect of LaFr26 in another way, we injected the peptide into the CA3 pyramidal cell layer of oraganotypic culture of rat hippocampus. Then the depolarizing effect is examined with anti-c-fos immunoreactivity, which is a marker protein of neuronal firings, 1 h after injection (Fig. 7). The c-fos immunoreactivity was induced at the site of injection, indicating the neuronal depolarizing effect in situ. Only background level of anti-c-fos immunoreactivity was observed in PBS-injected hippocampus (data not shown).

To test whether the depolarizing effect is a general phenomenon among pore-forming peptides or not, we added another pore-forming peptide, Css54, to the perfusate. The addition of Css54 (10 μM) depolarized the 56-3 cells (Fig. 8B). Similarly, the peptide induced burst firings and sustained depolarization in the hippocampal neuron (Fig. 8C). After the withdrawal of the Css54 peptide, the neuron was repolarized, restarted burst firings, and returned to initial status.

3.8. LaFr26 peptide induced pain related behavior

We used the hippocampal neuron as a model neuron, but it is unlikely that the hippocampal neurons are exposed to the spider venom. Instead, it is likely that peripheral sensory neurons are exposed to the venom when a spider bites mammals. If LaFr26 peptide induced firings as it does in the hippocampal neurons, it will induce pain sensation. To test this possibility, we tested the effect of the pore-forming peptides on pain sensation with hot-plate test. We measured latencies of paw withdrawal from the heated plate (55 °C) 5, 10, 15, and 20 min after planter injection of PBS, LaFr26, Css54, or ketorolac. The latencies were significantly shortened in LaFr6-injected mice 5 and 10 min after injection (Fig. 9), indicating that the pore-forming peptide induced thermal hyperalgesia. This hyperalgesic response was not-significant at 15 and 20 min. Similarly, another pore-forming peptide, Css54, induced hyperalgesia only at 5 min after injection. Ketorolac, which was used as an analgesic control, produced thermal hypoalgesia at 15 and 20 min post-injection, verifying the validity of our hot-plate test. This result shows the pain inducing effect of the pore-forming peptides, LaFr26 and Css54.

4. Discussion

In this report, we developed a GFP-based assay for Kir2.1 and found a venom peptide from the spider *Lachesana* sp., which decreased the GFP expression. The mechanism, by which the peptide decreased GFP expression, was shown to be pore-formation depending on hyperpolarization rather than the activation on Kir2.1 channel. The peptide depolarized the neurons and thereby produced pain in mice.

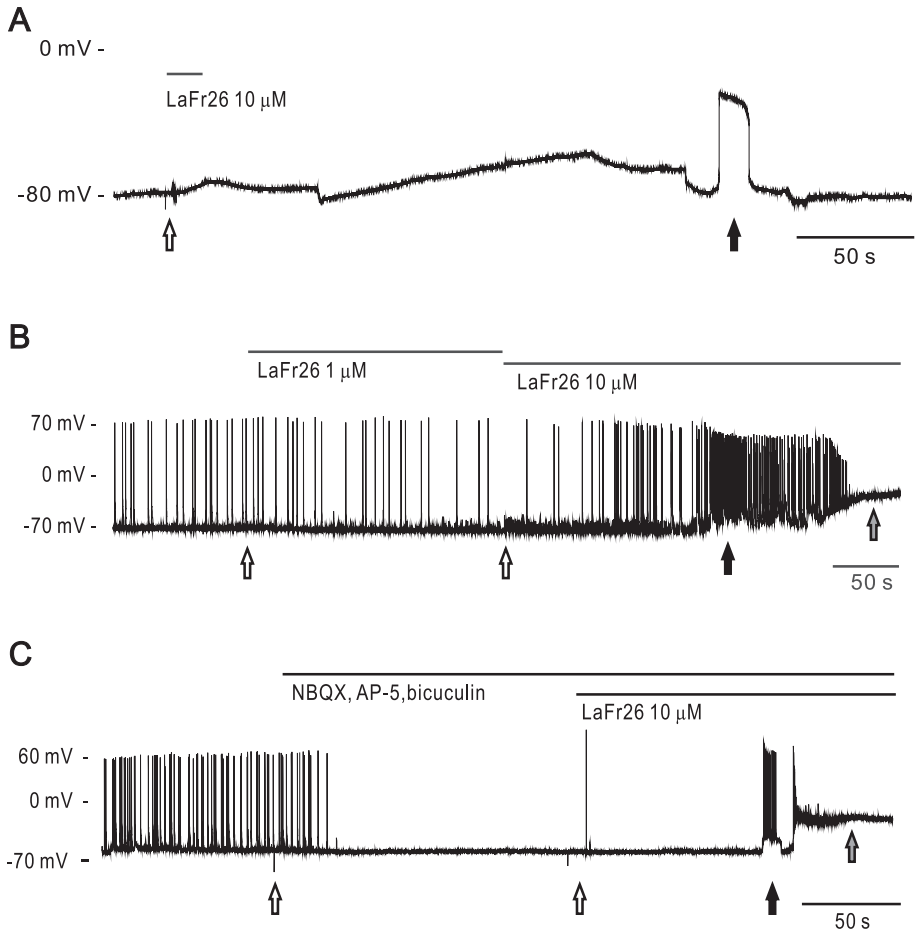

Fig. 6. LaFr26 induced depolarization and firing. (A) Change in whole-cell membrane potential by LaFr26 peptide. After a whole-cell patch-clamp was made, a 56-3 cell was held under current-clamp configuration, we applied 200 μl of 10 μM LaFr26 peptide (white arrow). The membrane potential was fluctuated over time, and then was abruptly depolarized and repolarized (black arrow). (B) Change in membrane potential of the CA1 pyramidal neuron by LaFr26. Whole cell current-clamp recording was made from a neuron in hippocampal slice culture. Then 1 and 10 μM LaFr26 peptide were sequentially applied (white arrows). The 10 μM peptide increased firing frequency (black arrow). Afterward, the neuron was inactivated because of the sustained depolarization (gray arrow). (C) Synaptic input-independent firing effect of LaFr26. When we applied antagonists for glutamate and $GABA_A$ receptors (white arrow in the left), the spontaneous firings were abolished. Even in the presence of the antagonists, the application of Fr26 peptide (10 μM, white arrow in the middle) induced burst firings (black arrow) and following sustained depolarization (gray arrow).

4.1. GFP-based assay

Despite their attractiveness as the targets, drug discovery for ion channel is slower than those for enzymes and receptors because of lack of the high-through-put assay [23]. Conventionally, screening of blockers has been done with patch-clamping, which is technically difficult and labor-intensive. The patch-clamping robots are costly. Therefore extensive efforts have been made to enable high-through-put assay for ion channels using radioactive ^{86}Rb [24], yeast [25,26], and fluorescent dye [27]. Here we provided another option that is simple and labor- and cost-saving. All procedures needed are transfection, addition of sample, and measurement of GFP fluorescence. Transfection with calcium-phosphate method is cost-saving. Reliability of the assay is shown by the shortness of error bars (Fig. 1 and 3). Indeed we successfully conducted a series of assays for various spiders and scorpions venom fractions, and found a GFP-decreasing activity (Fig. 2). Unexpectedly, the peptide we found here is a pore-forming peptide rather than Kir2.1 opener (Fig. 4). But the pore-forming activity was dependent on the Kir2.1 current (Fig. 3). These results verify the validity of our assay and indicate the usefulness of this assay even for the screening of pore-forming peptides.

We do not know detailed mechanisms of the GFP decrease by overexpressed Kir2.1 current. Fig. 1B shows that although the total cell numbers seem to be comparable (Phase contrast), the number of GFP-positive cells was reduced (GFP). Therefore the degenerative cells were probably detached during incubation and washed out by PBS washing before fixation. In addition, we found that the overexpression decreased cellular ATP level by half without affecting total cell number (Okada et al., submitted). Since small decrease in ATP level resulted in failure of protein synthesis [28], this decrease in ATP might be involved in at least in part.

4.2. Voltage-dependent pore-formation

We found a GFP-decreasing activity of LaFr26 venom (Fig. 2), and initially hypothesized that this peptide is an opener for Kir2.1 channel, because of the Ba^{2+}-sensitivity (Fig. 3B) and the lack of effect on mCherry expression (Fig. 3C). But, LaFr26 had no effect on Kir2.1 current (Fig. 4). Instead the peptide induced new current that was resistant to Ba^{2+} and lacked inward rectification or ion-selectivity. On the other hand, an identical peptide described earlier from *L. tarabaevi* has cytolytic, and pore-forming activities [18]. Consistently, we found that another pore-forming peptide, Css54, also induced similar current (Fig. 8). Furthermore, the peptide induced the current even in the naive 293T cells when they were voltage-clamped at −90 mV (Fig. 5). Thus, the induced current was attributable to the pore-formation by the LaFr26 peptide. The apparent Kir2.1 current-dependency of GFP-decreasing effect of the peptide seemed not to be dependent on Kir2.1

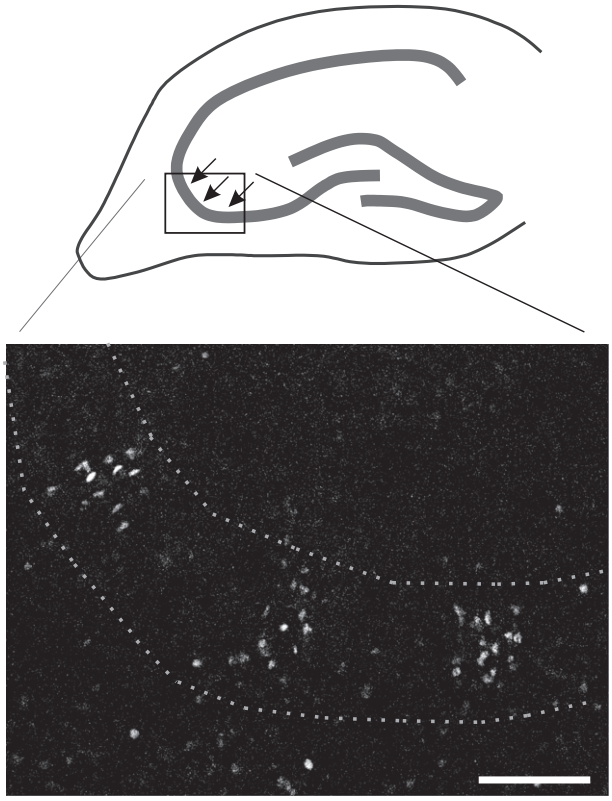

Fig. 7. LaFr26 induced c-fos protein in hippocampal neurons. Upper panel illustrates the structure of pyramidal and granule cell layers and site of injection (arrows). LaFr26 (3 μM, dissolved in PBS) was injected to three sites in the CA3 pyramidal cell layer of organotypic culture of rat hippocampus using Femtojet. The slice was fixed with 4% paraformaldehyde 1 h after injection and immunostained with anti-c-fos antibody. The immunoreaction was visualized with secondary antibody labeled with Alexa Fluor 568. Images of seven planes (533 × 400 × 15 μm, 2.5 μm interval) were stacked, and the pyramidal cell layer is indicated by dotted lines. Bar = 100 μm.

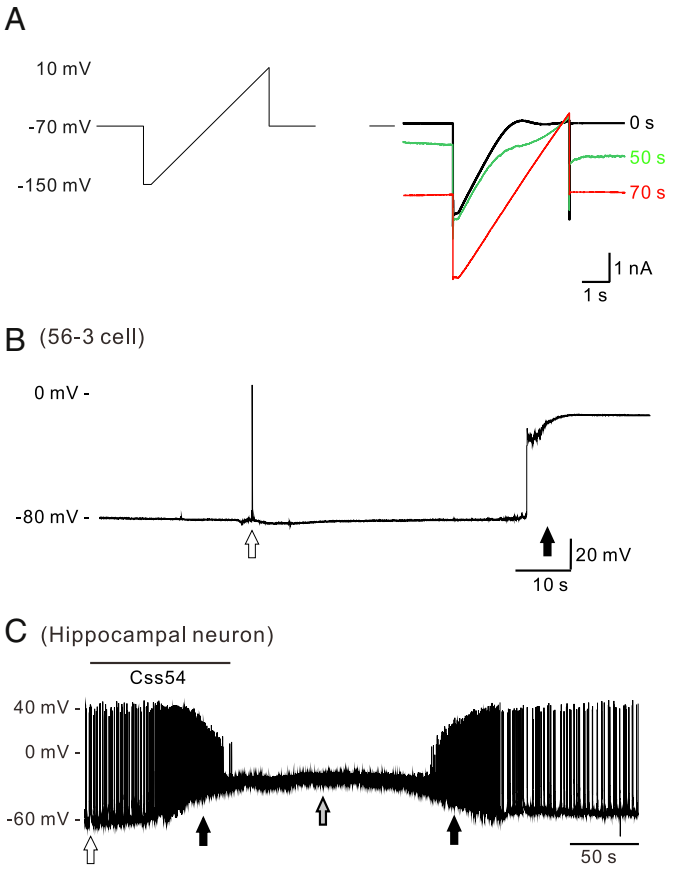

Fig. 8. Similar depolarizing and firing effects of Css54 peptide. (A) Similar induction of pore current by Css54 peptide in 56-3 cell. We made whole-cell patch-clamp from a 56-3 cell, and applied a ramp pulse (left panel). After the application of Css54 peptide, weakly rectified and non-rectifying currents were induced 50 and 70 s after, respectively. (B) Depolarization of 56-3 cell by Css54 peptide. Whole cell membrane potential was recorded from a 56-3 cell under current-clamp configuration. An application of Css54 (10 μM, white arrow) induced depolarization (black arrow). (C) Burst firings induced by Css54 peptide. We measured whole cell membrane potential from a hippocampal CA1 neuron. The application of Css54 (white arrow) also induced burst firings (black arrow in the left) and sustained depolarization (gray arrow). After the withdrawal of the Css54, the burst firings were induced again (black arrow in the right).

current itself, but on hyperpolarization. This was clearly indicated by the increase in the conductance of naive 293T, which was held at −90 mV (Fig. 5B and C). Furthermore, the TRITC-labeled peptide was selectively incorporated to Kir2.1-expressing cells (Fig. 5D, E, and F). Hyperpolarization-dependent pore-formation has been also reported in other pore-forming venom peptide [2]. In accordance with our results, Vassilevski et al. mentioned the higher dye leakage at a more negative potential of planar membrane by CIT1a peptide [19].

4.3. Induction of firing and pain

Bites and stings from arachnoid creatures can produce pain [29]. Several neural mechanisms have been proposed for the production of pain: blockade of K^+ channel, prolongation and activation of Na^+ channel [30,31], and activation of TRPV1 channel [32]. On the other hand, Yan and Adams (1998) reported that antimicrobial peptides from wolf spider venom depolarized the muscle membrane potential and resulted in reduction of excitatory junction potential in house fly larva [33]. In our results, the application of LaFr26 peptide depolarized 56-3 cells and induced burst firings of the hippocampal neurons in a synaptic input-independent way (Fig. 6). Similarly, Css54 also induced depolarization and firings (Fig. 8). The injection of the peptide induced anti-c-fos immunoreactivity in the CA3 pyramidal neurons (Fig. 7). In addition, injection of the peptide to paw of mouse induced hyperalgesic behavior (Fig. 9). Since LaFr26 or Css54 are components of the venom of spiders and scorpions, respectively, they seem to be involved in the pain from the bite or sting. This activity may be useful for the spider in deterring mammalian predators, in addition to the already proved antimicrobial

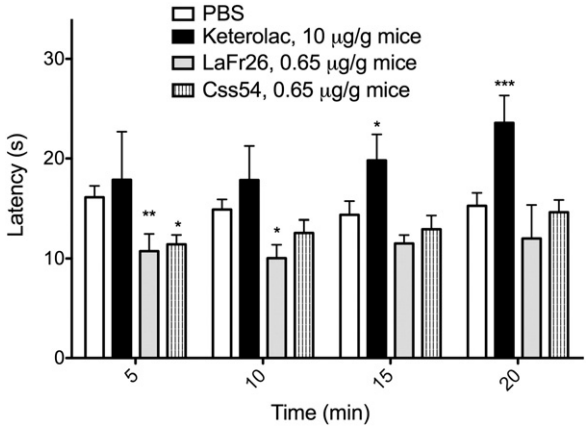

Fig. 9. Thermal hyperalgesic behavior following administration of LaFr26 and Css54. Latencies to withdraw the injected paws from the hot-plate were measured. The injections of LaFr26 shortened the latencies at 5 and 10 min after. Similarly, Css54 shortened the latency only at 5 min. Both pore-forming peptides induced rapid and short-lasting thermal hyperalgesia. Conversely, ketorolac elongated the latencies compared which those of PBS 15 and 20 min after. (* $p < 0.5$, ** $p < 0.01$, *** $p < 0.001$, $n = 5$).

Table 2
Names, spider species and amino acid sequences of pore forming peptides from spider venoms.

Name	Spider species	Amino acid sequences	aa	pI	%	References
Cupiennin 1a	*Cupiennius salei*	GFGALFKFLAKKVAKTVAKQAAKQGAKYVVNKQME	35	10.3	26.7	[2]
Cupennin 1b	*Cupiennius salei*	GFGSLFKFLAKKVAKTVAKQAAKQGAKYIANKQME	35	10.3	23.3	[2]
Cupennin 1c	*Cupiennius salei*	GFGSLFKFLAKKVAKTVAKQAAKQGAKYIANKQTE	35	10.3	23.3	[2]
Cupennin 1d	*Cupiennius salei*	GFGSLFKFLAKKVAKTVAKQAAKQGAKYVANKHME	35	10.3	23.3	[2]
Cytox1a(LaFr26)	*Lachesana tarabaevi*	GFFGNTWKKIKGKADKIMLKKAVKIMVKKEGISKEEAQAKVDAMSKKQIRLYLLKYYGKKALQKASEKL	69	10.1	100	[3]
Cytox1h	*Lachesana tarabaevi*	GFFGNAWKKIKGKAEKFFRKKAAKIIAKKEGITKEEAEAKVDTMSKKQIKVYLLKHYGKKALQKASEKL	69	10.1	79.7	[3]
Latarcin 1	*Lachesana tarabaevi*	SMWSGMWRRKLKKLRNALKKKLKGE	25	11.7	17.4	[5]
Latarcin 2	*Lachesana tarabaevi*	GLFGKLIKKFGRKAISYAVKKARGKH	26	11.3	38.5	[5]
Latarcin 3a	*Lachesana tarabaevi*	SWKSMAKKLKEYMEKLKQRA	20	10.1	30	[5]
Latarcin 3b	*Lachesana tarabaevi*	SWASMAKKLKEYMEKLKQRA	20	10.0	20	[5]
Latarcin 4a	*Lachesana tarabaevi*	GLKDKFKSMGEKLKQYIQTWKAKF	24	10.0	20	[5]
Latarcin 4b	*Lachesana tarabaevi*	SLKDKVKSMGEKLKQYIQTWKAKF	24	10.0	20	[5]
Latarcin 5	*Lachesana tarabaevi*	GFFGKMKEYFKKFGASFKRRFANLKKRL	28	11.1	17.7	[5]
Latarcin 6	*Lachesana tarabaevi*	QAFQTFKPDWNKIRYDAMKMQTSLGQMKKRFNL	33	10.3	34.8	[5]
Latarcin 7	*Lachesana tarabaevi*	GETFDKLKEKLKTFYQKLVEKAEDLKGDLKAKLS	34	10.3	18.2	[5]
Lycocitin 1	*Lycosa singoriensis*	GKLQAFLAKMKEIAAQTL	18	10.3	23.1	[6]
Lycocitin 2	*Lycosa singoriensis*	GRLQAFLAKMKEIAAQTL	18	10.0	23.1	[6]
Lycocitin 3	*Lycosa singoriensis*	KIKWFKTMKSLAKFLAKEQMKKHLGE	26	10.2	16.7	[6]
Lycosin-I	*Lycosa singorensis*	RKGWFKAMKSIAKFIAKEKLKEHL	24	10.4	25	[7]
LyeTx I	*Lycosa erythrognatha*	IWLTALKFLGKNLGKHLAKQQLAKL	25	10.6	25	[8]
Lycotoxin I	*Lycosa carolinensis*	IWLTALKFLGKHAAKHLAKQQLSKL	25	10.6	20	[9]
Lycotoxin II	*Lycosa carolinensis*	KIKWFKTMKSIAKFIAKEQMKKHLGGE	27	10.2	15.8	[9]
Oxt 4a	*Oxyopes takobius*	GIRCPKSWKCKAFKQRVLKRLLAMLRQHAF	30	11.6	21.4	[10]
Oxyopinin 1	*Oxyopes takobius*	FRGLAKLLKIGLKSFARVLKKVLPKAAKAGKALAKSMADENAIRQQNQ	48	11.3	32.4	[11]
Oxyopinin 2a	*Oxyopes takobius*	GKFSVFGKILRSIAKVFKGVGKVRKQFKTASDLDKNQ	37	10.8	19.2	[11]
Oxyopinin 2b	*Oxyopes takobius*	GKFSGFAKILKSIAKFFKGVGKVRKGFKEASDLDKNQ	37	10.3	19.2	[11]
Oxyopinin 2c	*Oxyopes takobius*	GKLSGISKVLRAIAKFFKGVGKARKQFKEASDLDKNQ	37	10.5	15.4	[11]
Oxyopinin 2d	*Oxyopes takobius*	GKFSVFSKILRSIAKVFKGVGKVRKGFKTASDLDKNQ	37	10.8	19.2	[11]

aa, number of amino acids; pI, isoelectric point; %, percentage of amino acid homology.

activity [5]. Furthermore, if these pore-forming peptides work on motor nerves of prey, it will facilitate their capture.

4.4. Sequence homology and evolution of the pore-forming peptides

A selection of cytolytic peptides from spider venoms is shown in Table 2. The first report of spider peptide structures with pore-forming activities was lycotoxins I and II, which were identified from the venom of the wolf spider *Lycosa carolinensis* [33]. Following them, the Cupiennins, Oxyopinins, Latarcins, LyeTx and Lycosins/Lycocitins from the spiders *Cupiennus salei*, *Oxyopes takiobus*, *L. tarabaevi*, *Lycosa erythrognath*, and finally from *Lycosa singoriensis*, respectively, were also reported with cytolytic properties [6,7,34]. Here only Cupiennins, Oxyopinins and the large Cyto-insectotoxins, including LaFr26, have

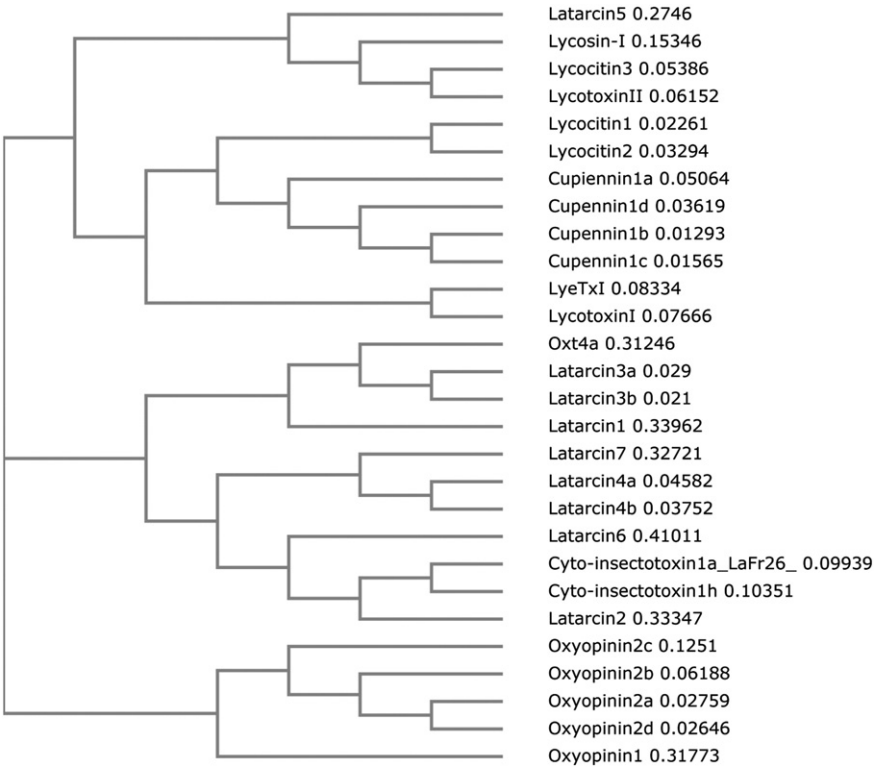

Fig. 10. Cladogram of LaFr26 and other pore-forming peptides.

been proved to be insecticidal and, as observed, with neurotoxic activity. Although the amino acid sequence identity among those peptides is quite low, they have the peculiarity of having a basic isoelectric point and a high content of hydrophobic residues (Table 2). Furthermore, an amino acid homology cladogram clearly shows that peptides are classified into four families (Lycotoxins, Cupiennins, Latarcins, and Oxyopinins), based on conserved specific peptide motifs (Fig. 10). Although latarcins 2 and 6 are shorter peptides, their evolutionary distances are the most related to LaFr26 (see Table 2). These peptides may have depolarizing and pain-inducing ability in common.

Acknowledgements

This work was supported by Strategic International Research Cooperative Program between JST and CONACyT.

References

[1] V. Quintero-Hernández, J. Jiménez-Vargas, G. Gurrola, H. Valdivia, L. Possani, Scorpion venom components that affect ion-channels function, Toxicon 76 (2013) 328–342.
[2] A. Vassilevski, S. Kozlov, E. Grishin, Molecular diversity of spider venom, Biochem. (Mosc.) 74 (2009) 1505–1534.
[3] N.R. Casewell, W. Wüster, F.J. Vonk, R.A. Harrison, B.G. Fry, Complex cocktails: the evolutionary novelty of venoms, Trends Ecol. Evol. 28 (2013) 219–229.
[4] A.H. Rowe, Y. Xiao, M.P. Rowe, T.R. Cummins, H.H. Zakon, Voltage-gated sodium channel in grasshopper mice defends against bark scorpion toxin, Science 342 (2013) 441–446.
[5] A.I. Kuzmenkov, I.M. Fedorova, A.A. Vassilevski, E.V. Grishin, Cysteine-rich toxins from Lachesana tarabaevi spider venom with amphiphilic C-terminal segments, Biochim Biophys Acta 2013 (1828) 724–731.
[6] G. Corzo, E. Villegas, F. Gomez-Lagunas, L.D. Possani, O.S. Belokoneva, T. Nakajima, Oxyopinins, large amphipathic peptides isolated from the venom of the wolf spider *Oxyopes kitabensis* with cytolytic properties and positive insecticidal cooperativity with spider neurotoxins, J. Biol. Chem. 277 (2002) 23627–23637.
[7] L. Kuhn-Nentwig, J. Muller, J. Schaller, A. Walz, M. Dathe, W. Nentwig, Cupiennin 1, a new family of highly basic antimicrobial peptides in the venom of the spider *Cupiennius salei* (Ctenidae), J. Biol. Chem. 277 (2002) 11208–11216.
[8] Y. Kubo, T.J. Baldwin, Y.N. Jan, L.Y. Jan, Primary structure and functional expression of a mouse inward rectifier potassium channel, Nature 362 (1993) 127–133.
[9] N.M. Plaster, R. Tawil, M. Tristani-Firouzi, S. Canún, S.d. Bendahhou, A. Tsunoda, M.R. Donaldson, S.T. Iannaccone, E. Brunt, R. Barohn, Mutations in Kir2. 1 cause the developmental and episodic electrical phenotypes of Andersen's syndrome, Cell 105 (2001) 511–519.
[10] M. Okada, H. Matsuda, Chronic lentiviral expression of inwardly rectifying K^+ channels (Kir2. 1) reduces neuronal activity and downregulates voltage-gated potassium currents in hippocampus, Neuroscience 156 (2008) 289–297.
[11] M. Okada, M. Kano, H. Matsuda, The degradation of the inwardly rectifying potassium channel, Kir2. 1, depends on the expression level: examination with fluorescent proteins, Brain Res. 1528 (2013) 8–19.
[12] G. Estrada, B.I. Garcia, E. Schiavon, E. Ortiz, S. Cestele, E. Wanke, L.D. Possani, G. Corzo, Four disulfide-bridged scorpion beta neurotoxin CssII: heterologous expression and proper folding in vitro, Biochim. Biophys. Acta (BBA) Gen. Subj. 1770 (2007) 1161–1168.
[13] F. Garcia, E. Villegas, G.P. Espino-Solis, A. Rodriguez, J.F. Paniagua-Solis, G. Sandoval-Lopez, L.D. Possani, G. Corzo, Antimicrobial peptides from arachnid venoms and their microbicidal activity in the presence of commercial antibiotics, J. Antibiot. 66 (2013) 3–10.
[14] A.B. Malmberg, A.W. Bannon, Models of nociception: hot-plate, tail-flick, and formalin tests in rodents, Curr. Protoc. Neurosci. 41 (8.9) (1999) 8.9.1–8.9.16.
[15] B. Sakmann, G. Trube, Conductance properties of single inwardly rectifying potassium channels in ventricular cells from guinea-pig heart, J. Physiol. 347 (1984) 641–657.
[16] M. Taglialatela, E. Ficker, B. Wible, A. Brown, C-terminus determinants for Mg^{2+} and polyamine block of the inward rectifier K+ channel IRK1, EMBO J. 14 (1995) 5532.
[17] P. Stanfield, N. Davies, P. Shelton, M. Sutcliffe, I. Khan, W. Brammar, E. Conley, A single aspartate residue is involved in both intrinsic gating and blockage by Mg^{2+} of the inward rectifier, IRK1, J. Physiol. 478 (1994) 1–6.
[18] S.A. Kozlov, A.A. Vassilevski, A.V. Feofanov, A.Y. Surovoy, D.V. Karpunin, E.V. Grishin, Latarcins, antimicrobial and cytolytic peptides from the venom of the spider *Lachesana tarabaevi* (Zodariidae) that exemplify biomolecular diversity, J. Biol. Chem. 281 (2006) 20983–20992.
[19] A. Vassilevski, S. Kozlov, O. Samsonova, N. Egorova, D. Karpunin, K. Pluzhnikov, A. Feofanov, E. Grishin, Cyto-insectotoxins, a novel class of cytolytic and insecticidal peptides from spider venom, Biochem. J. 411 (2008) 687–696.
[20] H. Matsuda, A. Saigusa, H. Irisawa, Ohmic conductance through the inwardly rectifying K channel and blocking by internal Mg2+, Nature 325 (1987) 156–159.
[21] B. Fakler, U. Brändle, E. Glowatzki, S. Weidemann, H.-P. Zenner, J. Ruppersberg, Strong voltage-dependent inward rectification of inward rectifier K^+ channels is caused by intracellular spermine, Cell 80 (1995) 149–154.
[22] T.C. Südhof, α-Latrotoxin and its receptors: neurexins and CIRL/latrophilins, Annu. Rev. Neurosci. 24 (2001) 933–962.
[23] J. Dunlop, M. Bowlby, R. Peri, D. Vasilyev, R. Arias, High-throughput electrophysiology: an emerging paradigm for ion-channel screening and physiology, Nat. Rev. Drug Discov. 7 (2008) 358–368.
[24] S. Daniel, L. Malkowitz, W. Hsuei-Chin, B. Beer, A.J. Blume, M.R. Ziai, Screening for potassium channel modulators by a high through-put 86-rubidium efflux assay in a 96-well microtiter plate, J. Pharmacol. Methods 25 (1991) 185–193.
[25] E. Zaks-Makhina, Y. Kim, E. Aizenman, E.S. Levitan, Novel neuroprotective K^+ channel inhibitor identified by high-throughput screening in yeast, Mol. Pharmacol. 65 (2004) 214–219.
[26] W. Tang, A. Ruknudin, W.-P. Yang, S.-Y. Shaw, A. Knickerbocker, S. Kurtz, Functional expression of a vertebrate inwardly rectifying K^+ channel in yeast, Mol. Biol. Cell 6 (1995) 1231–1240.
[27] L.M. Lewis, G. Bhave, B.A. Chauder, S. Banerjee, K.A. Lornsen, R. Redha, K. Fallen, C.W. Lindsley, C.D. Weaver, J.S. Denton, High-throughput screening reveals a small-molecule inhibitor of the renal outer medullary potassium channel and Kir7. 1, Mol. Pharmacol. 76 (2009) 1094–1103.
[28] H. Freudenberg, J. Mager, Studies on the mechanism of the inhibition of protein synthesis induced by intracellular ATP depletion, Biochimica et Biophysica Acta (BBA)-Nucleic Acids and Protein, Synthesis 232 (1971) 537–555.
[29] G.F. King, M.C. Hardy, Spider-venom peptides: structure, pharmacology, and potential for control of insect pests, Annu. Rev. Entomol. 58 (2013) 475–496.
[30] S. Cestele, Y. Qu, J.C. Rogers, H. Rochat, T. Scheuer, W.A. Catterall, Voltage sensor-trapping: enhanced activation of sodium channels by β-scorpion toxin bound to the S3–S4 loop in domain II, Neuron 21 (1998) 919–931.
[31] N.A. Valdez-Cruz, C.V. Batista, F.Z. Zamudio, F. Bosmans, J. Tytgat, L.D. Possani, Phaiodotoxin, a novel structural class of insect-toxin isolated from the venom of the Mexican scorpion *Anuroctonus phaiodactylus*, Eur. J. Biochem. 271 (2004) 4753–4761.
[32] J. Siemens, S. Zhou, R. Piskorowski, T. Nikai, E.A. Lumpkin, A.I. Basbaum, D. King, D. Julius, Spider toxins activate the capsaicin receptor to produce inflammatory pain, Nature 444 (2006) 208–212.
[33] L. Yan, M.E. Adams, Lycotoxins, antimicrobial peptides from venom of the wolf spider *Lycosa carolinensis*, J. Biol. Chem. 273 (1998) 2059–2066.
[34] S. Haeberli, L. Kuhn-Nentwig, J. Schaller, W. Nentwig, Characterisation of antibacterial activity of peptides isolated from the venom of the spider *Cupiennius salei* (Araneae: Ctenidae), Toxicon 38 (2000) 373–380.